Available online at www.sciencedirect.com
ScienceDirect
Polymer 49 (2008) 1800–1811
polymer
www.elsevier.com/locate/polymer

Fluorescence studies of pyrene-labelled, pH-responsive diblock copolymer micelles in aqueous solution

R. Rutkaite, L. Swanson*, Y. Li, S.P. Armes

Department of Chemistry, Dainton Building, University of Sheffield, Brook Hill, Sheffield S3 7HF, UK

Received 30 November 2007; received in revised form 28 January 2008; accepted 5 February 2008
Available online 8 February 2008

Abstract

Fluorescence spectroscopic techniques, and time-resolved anisotropy measurements (TRAMS) in particular, have provided valuable information regarding micelle formation in luminescently labelled pH-responsive diblock copolymers of 2-(diethylamino)ethyl methacrylate (DEA) and 2-(dimethylamino)ethyl methacrylate (DMA). A pyrenyl derivative, located at the DEA block, allowed motion of this site to be monitored *via* TRAMS in aqueous solution: a significant reduction in the mobility of this label was apparent at concentrations in excess of the critical micelle concentration, CMC, of the diblock copolymer. This is consistent with the labelled DEA block being located in the core of the micelles. At concentrations below the CMC, unimers were detected in solution. The micelle size estimated from TRAMS is approximately half of that determined from dynamic light scattering measurements. This suggests that the chain ends of the block copolymer are not ''frozen'' into position but that limited motion may occur due to fluidity within the micelle core. This is reasonable given the low T_g of the DEA block. Alternatively, a model is proposed which suggests that the interior of the micelle is a hard sphere, surrounded by flexible, fast-moving corona, which imparts little viscous drag on the core.

Keywords: Time-resolved anisotropy; Fluorescence; Diblock copolymer

1. Introduction

During the past two decades, luminescence spectroscopic techniques have been applied to a wide range of water-soluble/dispersible polymers with a view to characterize their aqueous solution behaviour [1–18]. Stimulus-responsive or ''smart'' polymers have featured particularly prominently [1–10,15–18]: chemists have been keen to understand the detailed molecular mechanisms by which the smart response is driven whether it be thermally, through changes in pH or salt concentration. A broad range of spectroscopic tools have been applied to the study of the conformational behaviour of water-soluble polymers. For example, simple changes in the vibrational fine structure of steady state spectra and the duration of the excited state fluorescence lifetime of both labels and probes have provided information on the magnitude of the smart response at the molecular level [1,4,6,9,10,15]. Fluorescence quenching experiments can probe the degree of ''compactness'' or ''openness'' of a polymer coil [1,5,6,9,10,15]. Such measurements have direct relevance for application of smart polymers as encapsulation aids for controlled release. Time-resolved anisotropy measurements (TRAMS) is a powerful method for probing the conformational behaviour of stimulus-responsive polymers since these provide information *directly* on macromolecular dynamics if a suitably labelled sample is used [3,8–10,15–17].

Synthesis of block copolymers containing hydrophobic or water-insoluble units with hydrophilic, solvated blocks allows exploitation of the amphiphilic nature of such systems. In many cases, spherical aggregates are formed from self-assembly of the insoluble blocks into micelles consisting of a hydrophobic core surrounded by a shell or corona of solvated blocks. Depending on the constituent components within the block, stimulus-responsive micelles can be formed. The use

* Corresponding author. Tel.: +44 114222 9564.
E-mail address: l.swanson@sheffield.ac.uk (L. Swanson).

0032-3861/$ - see front matter © 2008 Elsevier Ltd. All rights reserved.
doi:10.1016/j.polymer.2008.02.007

of luminescence spectroscopy has featured prominently in the study of block copolymer micelles [19–41]: valuable information regarding their nature and stability has been derived from fluorescence measurements.

Armes and co-workers have synthesized a series of pH-responsive diblock copolymers based on 2-(diethylamino)ethyl methacrylate (DEA) and 2-(dimethylamino)ethyl methacrylate (DMA) [42,43]. These two blocks have similar pK_a values of around pH 7.0–7.5. In acidic solution (pH < 6) the PDMA–PDEA diblock copolymer is molecularly dissolved as a cationic polyelectrolyte, since both blocks are highly protonated. On adjusting the solution pH to above 7, the DEA block gradually becomes hydrophobic, while the DMA block remains hydrophilic, even though the degrees of protonation of the two blocks are quite similar. This subtle difference leads to self-assembly to form PDEA–core micelles whose dimensions depend on the copolymer molecular weight and relative block composition. Such micellization is completely reversible: addition of acid leads to rapid micellar dissociation below pH 7.

In collaboration with Lee and Gast, the pH-induced micellization of one of these PDMA–PDEA diblock copolymers was studied in detail using dynamic light scattering, small-angle neutron scattering and fluorescence spectroscopy [38]. In the latter technique, pyrene was used as a probe molecule for characterizing the hydrophobic environment of the micelle cores. It was shown that the hydrophobicity of the PDEA chains in the micelle cores increased progressively as the solution pH was adjusted from pH 7 to pH 9. In the presence of electrolyte it was possible to observe both the individual unimer chains and the micelles under certain conditions. The critical micellization pH depended on both the copolymer concentration and also the background electrolyte concentration.

In the present manuscript we describe a detailed study of the aqueous solution behaviour of a pyrene-labelled PDEA–PDMA diblock copolymer using fluorescence spectroscopy.

We had two main aims in the current study.

(i) To probe the dilute aqueous solution behaviour of a luminescently labelled diblock copolymer, py-DEA_{30}–DMA_{130}, as a function of pH.
(ii) To monitor micellar self-assembly of Bz-DEA_{24}–DMA_{126} using py-DEA_{30}–DMA_{130} as a fluorescent probe.

The fact that PDEA is labelled allows this core forming [38,42] block to be monitored directly both in dilute and concentrated solutions. Applying fluorescence spectroscopic techniques such as TRAMS should allow estimation of the micelle dimensions and also provide information regarding the nature and microviscosity of the micelle cores. Use of a labelled copolymer offers specific advantages over those of a soluble probe: potentially the probe can be sequestered in both the hydrophobic core *and* in the more hydrophilic corona, while a label allows the tagged component (in the current work, the PDEA chain ends and consequently the micelle core) to be monitored directly. Since time-resolved anisotropy experiments have not been exploited to their full potential in the study of block copolymer micelles, we also provide data to critically assess the value of fluorescence TRAMS in monitoring micellar self-assembly.

2. Experimental

2.1. Materials

2-(Dimethylamino)ethyl methacrylate (DMA), 2-(diethylamino)ethyl methacrylate (DEA), pyrenemethanol, benzyl alcohol and potassium *tert*-butoxide (1.0 M in THF) were purchased from Aldrich. THF was dried with sodium wire for three days and subsequently refluxed in the presence of sodium. It was distilled under nitrogen just prior to use. All monomers were passed through basic alumina columns, stirred over calcium hydride for 24 h, stored at −9 °C, and distilled immediately prior to use. All other reagents were used as-received.

2.1.1. ^{1}H NMR spectroscopy

All ^{1}H NMR spectra were recorded at ambient temperature using a 300 MHz Bruker Avance DPX300 spectrometer either in $CDCl_3$ or CD_3OD.

2.1.2. Synthesis of the py-$PDEA_{30}$–$PDMA_{130}$ diblock copolymer

The pyrene-labelled $PDMA_{30}$–$PDEA_{130}$ diblock copolymer was prepared using oxyanionic polymerization. The general protocol was as follows. All glasswares were dried overnight at 150 °C, assembled hot under a nitrogen purge and then flamed out under dynamic vacuum to remove any residual surface moisture. Polymerizations were carried out at 50 °C in THF. The initiator precursor, 1-pyrenemethanol (0.300 g, 1.295 mmol), was added as a solid through a side-arm of the polymerization flask. Anhydrous THF (150 mL) was added to this flask using a double-tipped needle. To this solvent was added potassium *tert*-butoxide (1.30 mL of a 1.0 M THF solution, Aldrich), and this solution was stirred for approximately 30 min at 50 °C to ensure formation of the potassium 1-pyrenemethoxide initiator. Subsequently, freshly distilled DEA (6.5 mL, 6.0 g, 32.4 mmol, target Dp = 25) was added dropwise into the reaction flask, and the first-stage polymerization commenced. After 20 min, freshly distilled DMA (31.8 mL, 20.4 g, 130 mmol, target Dp = 100) was added dropwise to the living PDEA solution at 50 °C. After 2 h, the second-stage DMA polymerization was terminated with methanol. The crude diblock copolymer solution was then passed through a silica column and THF was removed under vacuum; the solid was washed three times with *n*-heptane to remove traces of unreacted pyrenemethanol initiator and also any PDEA homopolymer contamination. Finally, the purified copolymer was dried in a vacuum oven overnight at room temperature. The overall yield of isolated, purified strongly fluorescent diblock copolymer was approximately 21.0 g (80%). ^{1}H NMR analysis indicated that the actual diblock copolymer composition was py-$PDEA_{30}$–$PDMA_{130}$; GPC analysis (vs PMMA standards) gave $M_n = 7500$, $M_w = 9500$, $M_w/M_n = 1.27$.

2.1.3. Synthesis of the Bz-PDEA$_{24}$–PDMA$_{126}$ diblock copolymer for control experiments

The synthesis of the Bz-PDEA$_{24}$–PDMA$_{126}$ diblock copolymer was identical to that of the py-PDEA$_{24}$–PDMA$_{126}$ diblock copolymer except that benzyl alcohol was used as the initiator in place of 1-pyrenemethanol. Yield 29.1 g (85%). ^{1}H NMR analysis confirms that the real copolymer structure was Bz-PDEA$_{24}$–PDMA$_{126}$; GPC analysis (vs PMMA standards) shows $M_n = 5040$, $M_w = 6100$, $M_w/M_n = 1.21$.

2.1.4. Gel permeation chromatography (DMF eluent)

Molecular weights and molecular weight distributions of the diblock copolymers were assessed using a GPC set-up comprising three Polymer Laboratories' PL gel 5 μm mixed 'B' columns. Calibration was carried out using a series of near-monodisperse poly(methyl methacrylate) standards. The GPC eluent was HPLC grade DMF with 0.01 M LiBr, at a flow rate of 1.0 mL/min and the column temperature was set at 70 °C.

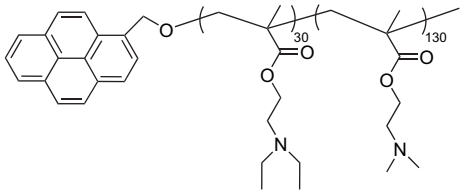

Chemical structure of the py-DEA$_{30}$–DMA$_{130}$ diblock copolymer

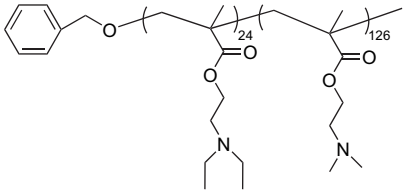

Chemical structure of the Bz-DEA$_{24}$–DMA$_{126}$ diblock copolymer

2.2. Instrumentation

2.2.1. Surface tensiometry

Surface tension measurements were conducted using a Kruss K1OST surface tensiometer (platinum ring method). Fig. 1 shows surface tension data as a function of Bz-PDEA$_{24}$–PDMA$_{126}$ concentration. The critical micelle concentration (CMC) was estimated as 0.007 ± 0.001 g/l from these data.

2.2.2. Dynamic light scattering

Dynamic light scattering measurements were carried out at 20 °C using a Brookhaven BI-200SM goniometer equipped with a BI-9000AT digital correlator and a solid-state laser (125 mV, $\lambda = 532$ nm) at a fixed scattering angle of 90°. The apparent intensity-average hydrodynamic diameter (D) and polydispersity index (μ_2/Γ^2) of micelles were evaluated from cumulant analysis of the experimental correlation function. The solution contained 1.0 g/l of diblock copolymer in 0.025 M sodium tetraborate. The solution temperature was controlled to within ±0.1 °C. An apparent hydrodynamic diameter of 25 nm was determined for the micelles formed from Bz-PDEA$_{24}$–PDMA$_{126}$.

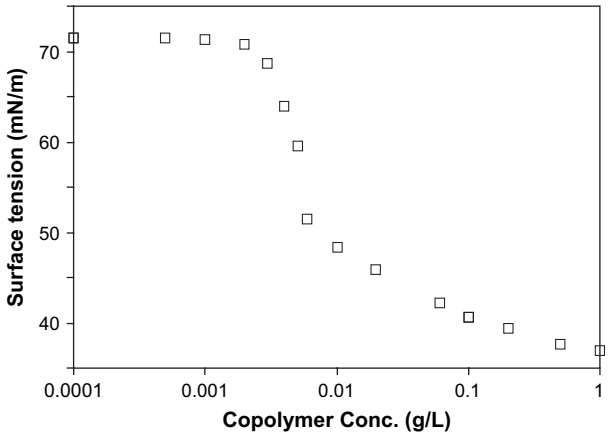

Fig. 1. Surface tension measurements as a function of Bz-PDEA$_{24}$–PDMA$_{126}$ concentration in aqueous solution.

2.2.3. Steady state fluorescence measurements

Fluorescence emission spectra were obtained using a Perkin–Elmer LS50b spectrometer. The excitation wavelength (λ_{ex}) was 340 nm and emission was sampled between 350 nm and 600 nm at 20 °C with slit widths of 2.5 nm for excitation and emission, respectively.

At a concentration of 0.01 g/l, which is in excess of the CMC, py-DEA$_{30}$–DMA$_{130}$ displays a broad featureless additional fluorescence band between 450 nm and 550 nm, which is characteristic of the pyrene excimer. Since intermolecular excimer formation or energy migration between labels could potentially interfere with the anisotropy experiments [44] the labelled polymer concentration was kept low (0.004 g/l) to minimise such interactions. A typical fluorescence emission spectrum is shown in Fig. 2 for py-DEA$_{30}$–DMA$_{130}$ (0.004 g/l) when part of a Bz-DEA$_{24}$–DMA$_{126}$ micelle at pH 9 in 0.025 M sodium tetraborate. Under these conditions,

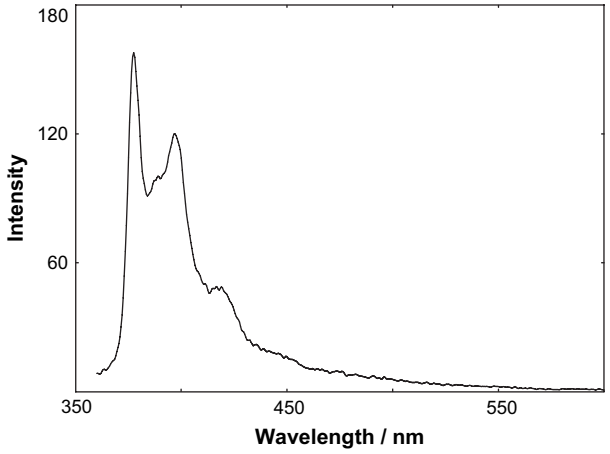

Fig. 2. Fluorescence emission spectrum for py-PDEA$_{30}$–PDMA$_{130}$ (0.004 g/l) and Bz-PDEA$_{24}$–PDMA$_{126}$ (1.0 g/l) at pH 9 in sodium tetraborate (0.025 M).

intermolecular interactions between chains are maximised but, by reference to Fig. 2, only emission from unassociated pyrene is present centred at 400 nm.

2.2.4. Time-resolved fluorescence measurements

Fluorescence lifetimes were determined using an Edinburgh Instruments 199 spectrometer operating on the time-correlated single photon counting principle. An IBH Horiba Jobin Yvon diode based megahertz nanoled (Nanoled-16) was used as the excitation source with a full width half maximum pulse width of 800 ps and peak response at 340 nm. The total response of the detection channel which included a fast photomultiplier (Hamamatsu R3235) was *ca.* 1.2 ns. The instrument was modified through addition of a second detection channel to allow time-resolved anisotropy measurements (TRAMS) to be made. This channel was equipped with a ''toggling'' device, which periodically switched the plane of polarization of the analyser and simultaneously addressed the detector signals to a designated memory segment in the multichannel analyser. This allowed accumulation of the parallel $[i_{\parallel}(t)]$ and perpendicular $[i_{\perp}(t)]$ components, respectively, which are necessary to derive the anisotropy decay, $r(t)$ as in Eq. (1).

$$r(t) = \frac{i_{\parallel}(t) - iG_{\perp}(t)}{i_{\parallel}(t) + 2Gi_{\perp}(t)} = \frac{d(t)}{s(t)} \tag{1}$$

where $d(t)$ and $s(t)$ are the difference and sum functions, respectively. G is a factor designed [45] to correct for differences in transmission and detection efficiencies in the determination of $i_{\parallel}(t)$ and $i_{\perp}(t)$. Combinations of broad band-pass and interference filters to isolate fluorescence at appropriate wavelengths resulted in G factors of unity in experiments involving the current instrument. (G was estimated by comparison of the emission intensities analysed in planes parallel and perpendicular, respectively, to the plane of *horizontally* polarized excitation.)

In the current work we have favoured the use of impulse reconvolution to analyse the time-resolved anisotropy data: impulse reconvolution [46] involves analysis of $s(t)$ by a statistically adequate model function. The ''best fit'' to $s(t)$ is represented by an impulse response function which, in combination with an assumed model for the anisotropy decay may be used in an iterative least squares reconvolution procedure to fit $d(t)$. This fit is optimized by varying the fitting parameters which allows derivation of relaxation data for the process under investigation.

Full details of the TRAMS experiment and associated analytical procedures have been described elsewhere [47].

For all time-resolved experiments the λ_{ex} was 340 nm and emission was isolated at 400 nm via an interference filter.

Due to the low concentration of labelled block copolymer (0.004 g/l) and the fact that quenching of the fluorescence occurred at pH values greater than 7, long data accumulation times ($\sim$12 h) were necessary to achieve a minimum of 10,000 counts in the peak of $i_{\parallel}(t)$.

2.3. Solutions for spectroscopic analyses

Air saturated solutions contained labelled diblock copolymer (py-DEA_{30}–DMA_{130}) at a concentration of 0.004 g/l and unlabelled sample (Bz-DEA_{24}–DMA_{126}) was varied between 0 g/l and 1.0 g/l. The pH was varied by potentiometric titration as previously described [38].

For Stern–Volmer experiments using NaI as a quencher, $Na_2SO_3^{2-}$ (4×10^{-3} M) was added to the solution to prevent oxidation of iodide to iodine.

3. Results and discussion

3.1. Dilute solution behaviour of PDEA-b-PDMA via fluorescence techniques

To monitor the dilute aqueous solution behaviour of py-DEA_{30}–DMA_{130} a nominal concentration of 0.004 g/l was used in all fluorescence measurements which is below the CMC derived from surface tension measurements (see Fig. 1). These conditions were employed to minimise any intermolecular interactions between fluorescent labels which could potentially interfere [44] with time-resolved anisotropy measurements, in particular.

3.1.1. Excited state lifetime measurements

The excited state fluorescence lifetime (τ_f) of pyrene is sensitive [48] to the polarity of its microenvironment. Indeed, τ_f data, coupled with information derived from the analysis of vibrational fine structure of the fluorescence emission, have been used to investigate the conformational behaviour of pH-responsive, water-soluble polymers [1,3,4,6,10,15,49,50]. Previous work on PDEA-*b*-PDMA block copolymer micelles has utilised the sensitivity of pyrene (present as a probe) to its environment: the hydrophobicity of the micellar core increased on adjusting the pH from 7 to 9 [38]. These data were consistent with the formation of micelles as the PDEA and PDMA blocks become progressively deprotonated. The current work differs from previous studies [38] in that the pyrene label is covalently attached to PDEA-*b*-PDMA at the PDEA chain end. This strategy was adopted to assess whether the label could provide any information regarding its environment via its fluorescence lifetime and hence the conformational state of the block copolymer at various pH conditions.

Fig. 3a shows an example of a fluorescence decay curve from py-$PDEA_{30}$–$PDMA_{130}$ (0.004 g/l) at pH 1.25. In the current work, the excited state lifetime, τ_f, was derived by modelling the time-resolved fluorescence data to sums of exponentials of the form of Eq. (2).

$$I(t) = \sum_i A_i \exp(-t/\tau_i) \tag{2}$$

where A_i represents the amount of each component (τ_i) present. Initially a single exponential function with $i = 1$, as in Eq. (2), was used to fit the curve (see Fig. 3a). Clearly, such a model is inappropriate for the current data: the χ^2 value is

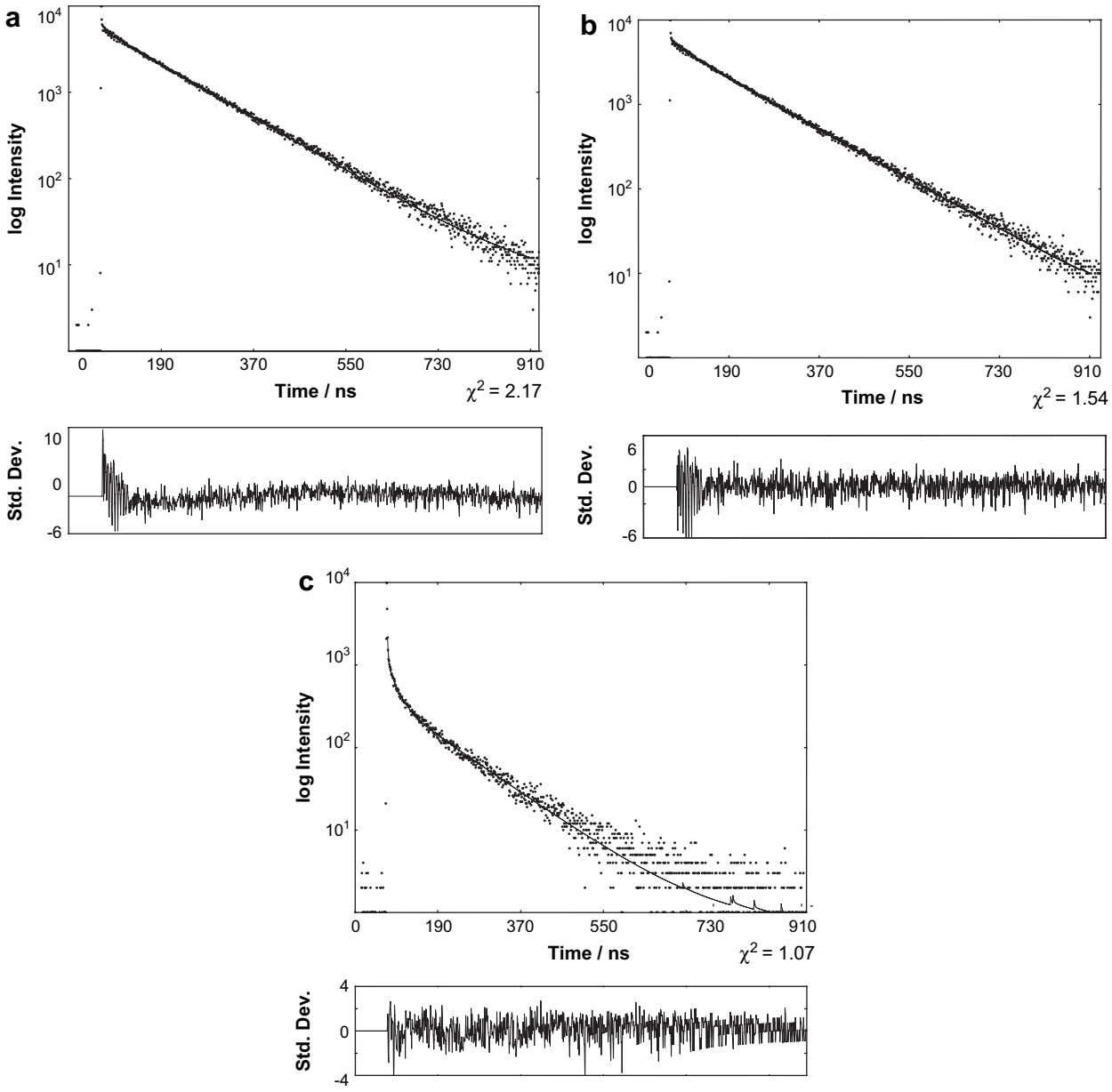

Fig. 3. (a) Decay of fluorescence from py-PDEA$_{30}$–PDMA$_{130}$ (0.004 g/l) at pH 1.25 with "best fit" to a single exponential model function and residuals ($\lambda_{ex} = 340$ nm; $\lambda_{em} = 400$ nm). (b) Decay of fluorescence from py-PDEA$_{30}$–PDMA$_{130}$ (0.004 g/l) at pH 1.25 with "best fit" to a triple exponential model function and residuals ($\lambda_{ex} = 340$ nm; $\lambda_{em} = 400$ nm). (c) Decay of fluorescence from py-PDEA$_{30}$–PDMA$_{130}$ (0.004 g/l) at pH 9.5 with "best fit" to a triple exponential model function and residuals ($\lambda_{ex} = 340$ nm; $\lambda_{em} = 400$ nm).

2.17 (χ^2 should be close to unity for a good fit) and the residuals are non-randomly distributed, particularly at early times in the decay. The time-resolved data are best described (see Fig. 3b) by use of a triple exponential function (with $i = 3$ in Eq. (2)). The random distribution of residuals around zero (see Fig. 3b) and the low value of χ^2 provide statistical confidence in the quality of the fit. Such complexity in decay kinetics appears to be a common feature of fluorescently labelled water-soluble polymers and has previously been attributed to the heterogeneous range of environments accessed by the fluorophore [8,13,15,49–51]. At pH 9, the decay becomes markedly non-exponential (see Fig. 3c) and the duration of fluorescence is much less than that observed at pH 1.25 (see Fig. 3b). Presumably this trend reflects the fact that quenching occurs at high pH as the deprotonated tertiary amine groups come into contact with the fluorescent label. (Tertiary amines are known to be efficient fluorescence quenchers [52,53].)

Although we cannot, with confidence, assign the three exponential terms to specific physical species, valuable information can nonetheless be derived from the data by calculating an average fluorescence lifetime, $\langle \tau_f \rangle$ *via* Eq. (3).

$$\langle \tau_f \rangle = \frac{\sum I_i \tau_i^2}{\sum I_i \tau_i} \tag{3}$$

This form of data treatment has proven particularly informative in our previous studies of the conformational behaviour

of stimulus-responsive polymers [8,10,15,49,50]. The $\langle\tau_f\rangle$ values obtained for py-DEA$_{30}$–DMA$_{130}$ from this form of analysis for all pH values are listed in Table 1. Clearly, $\langle\tau_f\rangle$ decreases monotonously with increasing pH, from 127.8 ns to 70.5 ns. This is contrary to expectation: previous fluorescence measurements using a methyl orange probe confirmed [54] that the homopolymer, PDMA, changes from an extended structure at low pH to a compact coil at high pH [55,56]. From our experience of the conformational behaviour of smart polymers using a pyrene probe [8,15,49,50], and with reference to the literature [1,4,6], it was expected that the fluorescence lifetime of the label should increase assuming that the DMA component induces a chain collapse in the block copolymer. (Under these circumstances the fluorophore would experience a more hydrophobic environment). The current data do not follow this trend. Deprotonation of the tertiary amine units occurs at high pH [38], which presumably then act as efficient contact quenchers [52,53] of the excited state of the pyrene label. As the degree of deprotonation increases with increasing pH, this leads to a higher quenching efficiency and a resultant decrease in $\langle\tau_f\rangle$. Consequently, the current lifetime data are somewhat inconclusive as regards the conformation of the block copolymer. Thus additional fluorescence techniques (described in the subsequent sections) were employed to provide definitive evidence of the conformational state of py-DEA$_{30}$–DMA$_{130}$ under dilute aqueous solution conditions.

3.1.2. Fluorescence quenching

Fluorescence quenching experiments can provide information concerning the degree of accessibility of a quencher to a fluorophore. If the process is governed by Stern–Volmer kinetics, as described in Eq. (4),

$$\tau^0/\tau = 1 + k_q\tau^0[Q] \quad (4)$$

then it is possible to derive the bimolecular quenching constant, k_q, which is a measure of the efficiency of deactivation of the excited state by the quencher, Q. (τ^0 and τ are the fluorescence lifetimes in the absence and presence of some concentration of quencher, Q.) Provided that experiments are conducted using suitably labelled samples, k_q in turn will provide information on the degree of "openness" of a polymer chain in solution [1–6,9,10,15,50,51].

The rationale for the current Stern–Volmer experiments was to determine the ease of access into the block copolymer of two water-soluble quenchers in dilute aqueous solution: nitromethane, which is an example of a neutral quencher and iodide, which is anionic. It was hoped that these experiments would provide information about the degree of intramolecular coiling of the block copolymer at both low and high pH.

Fluorescence decays were measured as a function of quencher concentration and over a wide range of pH conditions. The decays were observed to be complex, irrespective of the quencher type, concentration or pH condition, requiring a minimum of three exponential terms (as in Eq. (2)) for an adequate fit on statistical grounds. An average lifetime was subsequently calculated by Eq. (3) which allowed k_q to be derived from Eq. (4). All Stern–Volmer analyses in the current work were carried out in this manner.

Fig. 4 shows example Stern–Volmer plots acquired at pH values 1.45, 4.9, 8.0 and 9.5, using NaI as the quencher. Very complex quenching behaviour was observed from py-PDEA$_{30}$–PDMA$_{130}$ in dilute aqueous solution below pH 6. Just over 50% protonation of the PDEA-*b*-PDMA sample is known [38] to occur at pH 7.2 while above pH 8 this reduces to less than 10%. This is consistent with the Stern–Volmer data shown in Fig. 4: linear plots are obtained at higher pH since dynamic iodide quenching should occur under these conditions. The k_q values derived are *ca.* 3×10^9 mol^{-1} dm^3 s^{-1} for pH 8 and 9.5, respectively. Such quenching constants are consistent with a partially coiled structure, or certainly with hindered access of the I^- to the excited state, since the quenching efficiency is reduced to that expected (*ca.* 8×10^9 mol^{-1} dm^3 s^{-1}) for a diffusion-controlled process. Further examination of Fig. 4 reveals that two regions of the plot are clearly evident at pH 1.45 and 4.9, respectively: at low [NaI], a steep gradient occurs. The k_q value associated with this concentration regime is estimated as 1.6×10^{10} mol^{-1} dm^3 s^{-1}, which is greater than for the diffusion-controlled process. Presumably, the I^- acts as a counter

Table 1
Average fluorescence lifetime, $\langle\tau_f\rangle$, for aqueous solutions of py-PDEA$_{30}$–PDMA$_{130}$ (0.004 g/l) as a function of pH and Bz-PDEA$_{24}$–PDMA$_{126}$ concentration at 20 °C

pH	[Bz-PDEA$_{24}$–PDMA$_{126}$] (g/l)	$\langle\tau_f\rangle$ (ns)
1.45	0	127.8
4.9	0	111.3
8	0	97.4
9.5	0	70.5
9 (buffered)	0	61.5
1.25	1.0	123.2
5.2	1.0	107.3
8	1.0	48.6
9.5	1.0	27.1
9 (buffered)	1.0	32.7

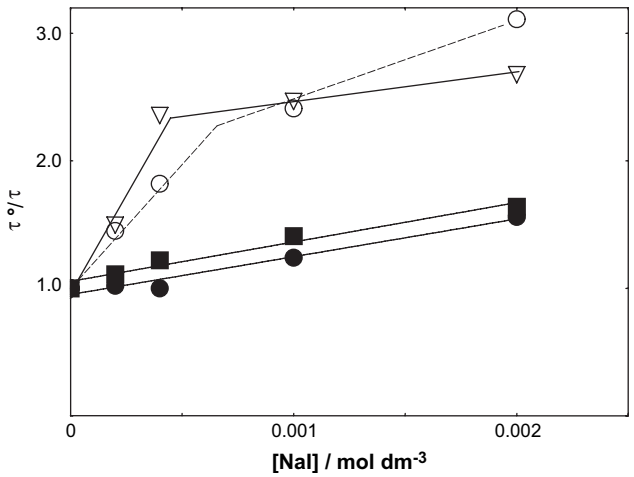

Fig. 4. Stern–Volmer plots for the quenching of fluorescence from aqueous solutions of py-PDEA$_{30}$–PDMA$_{130}$ (0.004 g/l) by NaI at pH 1.45 [▽], 4.9 [○], 8 [■] and 9.5 [●].

ion for the protonated amines of the copolymer, which creates a high local concentration of quencher (much greater than that of the nominal bulk I^- concentration added to the solution). Consequently, an extremely high k_q value is derived *via* the Stern–Volmer relationship (Eq. (4)). Such complex quenching behaviour has been observed previously for other ionised water-soluble copolymer/quencher combinations [1,2,5,6,9,51,57,58].

Further consideration of Fig. 4 reveals that once iodide saturation of the protonated amines occurs a less steep region of the Stern–Volmer plot is evident at pH 1.45 and 4.9. Normal diffusion-controlled quenching by I^- occurs in this concentration regime with a characteristic k_q value of $\sim 5.5 \times 10^9$ mol^{-1} dm^3 s^{-1}. The current Stern–Volmer experiments using I^- reveal the degree of protonation of the py-PDEA$_{30}$–PDMA$_{130}$ sample across the pH range.

Fig. 5 shows typical Stern–Volmer plots for py-PDEA$_{30}$–PDMA$_{130}$ using nitromethane as a quencher at pH 1.25 and 9.5. Clearly, "normal" linear plots are obtained at the two pH extremes, which is in contrast to the behaviour observed when NaI was used as a quencher. The k_q value obtained at pH 1.25 following quenching with nitromethane is 3.24×10^9 mol^{-1} dm^3 s^{-1} (see Table 2). This value is just under half that reported [10] for the expanded conformation of an ACE-labelled poly(*N*-isopropylacrylamide), PNIPAM, sample with the same quencher at 25 °C. The reduction in quenching efficiency observed for the current sample when compared to that of the open chain state of PNIPAM indicates that the quencher may be inhibited by the protonated amine units as it tries to access the excited state. A slight reduction in k_q occurs when the Stern–Volmer experiment is repeated for py-PDEA$_{30}$–PDMA$_{130}$ at pH 9.5: k_q is *ca.* 1.52×10^9 mol^{-1} dm^3 s^{-1} (see Table 2). The decrease in k_q observed upon increasing pH reflects hindered access to the excited state by nitromethane which could be indicative of a slight contraction of the block copolymer coil. It was hoped that time-resolved anisotropy measurements, discussed in the next section, would provide definitive information regarding

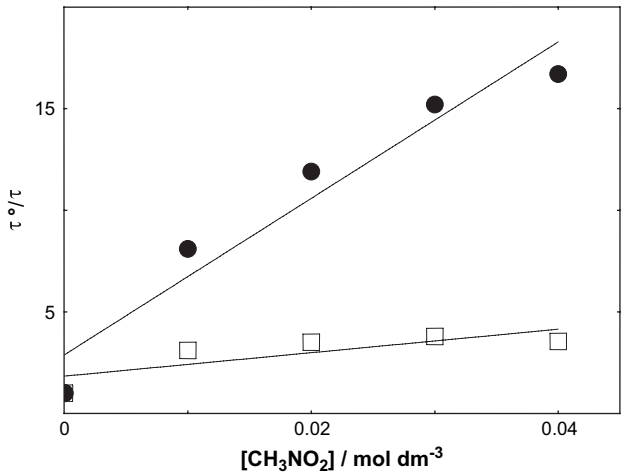

Fig. 5. Stern–Volmer plots for the quenching of fluorescence from aqueous solutions of py-PDEA$_{30}$–PDMA$_{130}$ (0.004 g/l) by nitromethane at pH 1.25 [●] and 9.5 [□].

Table 2
Rate constants for the quenching of fluorescence from aqueous solutions of py-PDEA$_{30}$–PDMA$_{130}$ (0.004 g/l) by nitromethane as a function of pH and Bz-PDEA$_{24}$–PDMA$_{126}$ concentration at 20 °C

[Bz-PDEA$_{24}$–PDMA$_{126}$] (g/l)	pH	$k_q \times 10^9$ (mol^{-1} dm^3 s^{-1})
0	1.25	3.24 ± 0.15
0	9.5	1.52 ± 0.04
0	9 (buffer)	0.20 ± 0.01
1.0	1.25	3.51 ± 0.15
1.0	9.5	1.0 ± 0.04
1.0	9 (buffer)	0.17 ± 0.01

the conformational state of the block copolymer in dilute solution at both low and high pH.

3.1.3. Time-resolved anisotropy measurements

Over the past two decades, time-resolved anisotropy measurements (TRAMS) have proven to be an invaluable tool for probing polymer dynamics in aqueous solution [3,8–10,15–17,49,50]. Macromolecules that exhibit smart behaviour (i.e. can respond to an external stimulus such as temperature or pH by either a chain collapse or expansion) have featured prominently in these investigations: TRAMS offer the opportunity of monitoring the general reduction in segmental mobility which occurs upon contraction of a responsive polymer into a globular state and, as such, can provide information which is pertinent in consideration of such materials for controlled release applications. In the current work, since the ends of the PDEA chains are labelled with pyrenyl units and these chains form the micelle cores [38,42] then TRAMS should allow probing, at the molecular level, of the micellization process itself.

A more detailed discussion of the theory of TRAMS and methods of data analyses is given elsewhere [47]: we cover only the salient features here. Following excitation with vertically polarized light, a distribution of fluorophores whose transition vectors for the absorption process are vertically aligned will be photoselected, creating an excited state population, which possesses a degree of anisotropy (r) or optical order, in an otherwise isotropic distribution of fluorophores. In a time-resolved experiment, the time-dependent intensities, $i_{\|}(t)$ and $i_{\perp}(t)$, are measured in planes parallel and perpendicular, respectively, to the plane of polarization of the incident radiation. These parameters are subsequently combined, *via* Eq. (1), to generate the decay of anisotropy, $r(t)$.

Loss of r will result through molecular motion within the excited state fluorescence lifetime (τ_f) until the photoselected population achieves an isotropic orientation. Assuming that the anisotropy decays following a simple, single relaxation mechanism it will be described by Eq. (5).

$$r(t) = r_0 \exp(-t/\tau_c) \tag{5}$$

where τ_c, the correlation time, characterizes the rate of motion under study. In the current work, since the chain ends of the block copolymer are labelled, TRAMS should allow the mobility of these sites to be monitored *via* the resulting τ_c.

The dilute solution behaviour of py-DEA_{30}–DMA_{130} was examined initially below its CMC *via* TRAMS. The copolymer dynamics were extremely rapid under these conditions, irrespective of the pH of the solution. Consequently, it was necessary to analyse the data *via* impulse reconvolution [46], since this allows the perturbing effects of the excitation pulse to be mathematically removed from the data. (Analysis of anisotropy data can become particularly problematic if the motion under study is comparable to the width of the excitation pulse [47].)

Fig. 6a shows the difference decay, $d(t)$, of py-DEA_{30}–DMA_{130} at a concentration of 0.004 g/l at pH 9. It is apparent that $d(t)$ decays rapidly to zero within the timescale accessed in the current study. Such behaviour is indicative of very rapid motion of the chain ends and is consistent with an open chain, expanded conformation. A τ_c of *ca.* 1.8 ± 0.2 ns results from impulse reconvolution [46] analysis of the decay using a single exponential model as described by Eq. (5). Further examination of Fig. 6a reveals that the fitting statistics, in the form of the residuals and χ^2, both indicate that the model is appropriate: the residuals are randomly distributed about zero with a χ^2 of 1.3.

At pH 1.45, a τ_c of 2.7 ± 0.3 ns was derived *via* impulse reconvolution [46] of $d(t)$ using a single exponential model. This would indicate that the block copolymer adopts a similar conformation to that at pH 9.

A word of caution should, however, be acknowledged at this point. Ideally, τ_f of the label should be closely matched to the timescale of the motion (τ_c) under study [47]. This is not the case with the current py-$PDEA_{30}$–$PDMA_{130}$ sample: τ_c is *ca.* 2 ns while $\langle\tau_f\rangle$ varies between *ca.* 128 ns and *ca.* 71 ns depending on the pH. In order to probe the fast motion of the chain ends, a shorter-lived label (such as an anthracene or naphthalene derivative) would be preferable. However, in the current context, the main driving force behind the study was to monitor micellar self-assembly at higher block copolymer concentration. Under these conditions, since a dramatic reduction in the mobility of the chain ends would be expected and a concomitant increase in τ_c anticipated, use of a label such as pyrene, with a relatively long-lived lifetime is not unreasonable. Despite the limitations of the current time-resolved anisotropy experiments in probing the dilute solution behaviour of py-$PDEA_{30}$–$PDMA_{130}$, it is tempting to conclude that no discernable change in conformation occurs: certainly the chain ends experience no restriction in mobility as the pH is increased. Given that changes in lifetime and quenching behaviour occur as a function of pH, it is likely that these merely reflect deprotonation of the block copolymer, since this would have an impact on the local environment of the label.

3.2. Effect of the presence of sodium tetraborate on the dilute solution behaviour of py-$PDEA_{30}$–$PDMA_{130}$

Since the copolymer forms stable micelles at pH 9 in the presence of sodium tetraborate buffer, we have chosen these conditions to test the applicability of fluorescence techniques, and TRAMS in particular, to the study of micellization. Consequently, in order to assess the effect of the presence of buffer on the conformation of py-$PDEA_{30}$–$PDMA_{130}$ under dilute solution conditions (below the CMC), we have used various fluorescence spectroscopic tools as outlined in the following sections.

3.2.1. Excited state lifetime data

Inspection of Table 1 reveals that $\langle\tau_f\rangle$ of py-$PDEA_{30}$–$PDMA_{130}$ (0.004 g/l) at pH 9 in 0.025 M sodium tetraborate

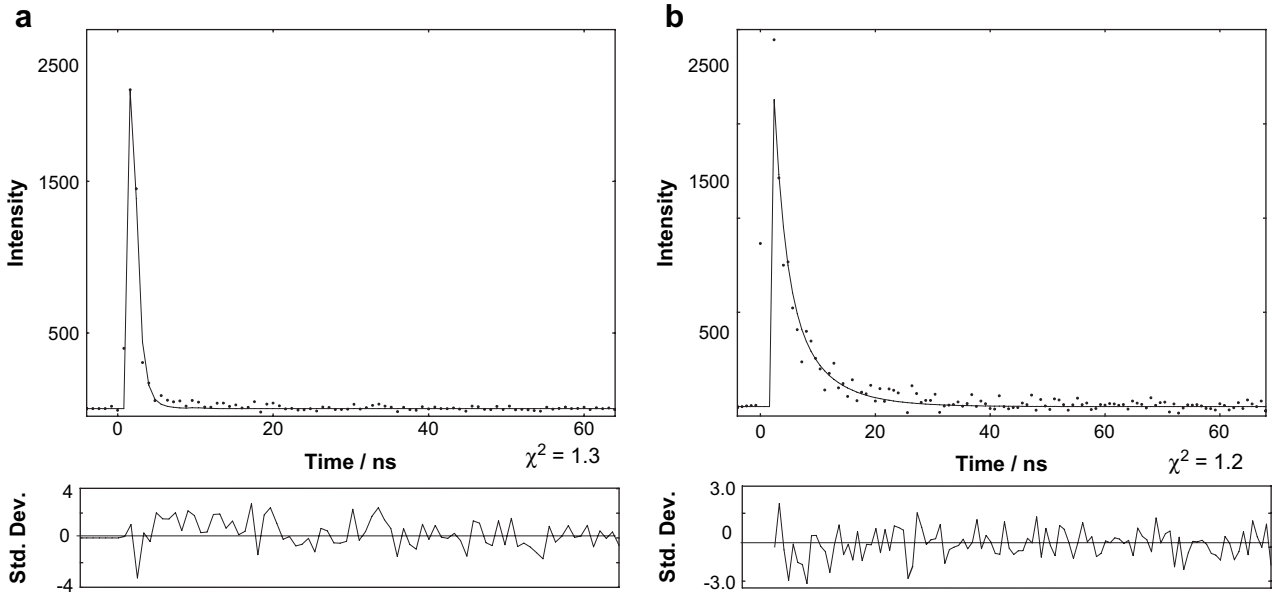

Fig. 6. (a) Difference curve, $d(t)$, single exponential fit and distribution of residuals following impulse reconvolution fitting to fluorescence data for py-$PDEA_{30}$–$PDMA_{130}$ (0.004 g/l) at pH 9. (b) Difference curve, $d(t)$, single exponential fit and distribution of residuals following impulse reconvolution fitting to fluorescence data for py-$PDEA_{30}$–$PDMA_{130}$ (0.004 g/l) at pH 9 in sodium tetraborate (0.025 M).

is *ca*. 62 ns. This represents a reduction of ~9 ns compared to that in the absence of buffer and is consistent with a more compact coil under these conditions. The increased degree of quenching indicates that the label is brought into closer contact with the tertiary amine groups in the presence of buffer. Since tertiary amines are known [52,53] to be efficient fluorescence quenchers, a reduction in τ_f would be expected. To prove the hypothesis that the amine units quench the fluorescence of the labelled block copolymer triethylamine was added (at various concentrations) to py-PDEA$_{30}$–PDMA$_{130}$ (0.004 g/l) in aqueous solution: a significant degree of quenching was indeed observed with a k_q value of *ca*. 0.2×10^9 mol^{-1} dm^3 s^{-1}.

3.2.2. Stern–Volmer quenching experiments

To further investigate the effect of buffer on the conformation of py-PDEA$_{30}$–PDMA$_{130}$ under dilute solution conditions, we have repeated the Stern–Volmer experiment in the presence of 0.025 M sodium tetraborate using nitromethane as a quencher. The bimolecular quenching constant derived from fluorescence lifetime data is 0.2×10^9 mol^{-1} dm^3 s^{-1} (see Table 2). This is almost an order of magnitude less than that in the absence of buffer and infers that the quencher experiences greater difficulty in accessing the pyrenyl-labelled chain ends. This provides additional evidence that the buffer may induce a change in the block copolymer conformation in dilute solution. However, these data should be viewed with an element of caution at this point: it has been acknowledged previously [14,59] that there is potential in water-soluble systems for partitioning of the quencher between the aqueous phase and the hydrophobic regions of the polymer coil. Addition of tetraborate buffer to the current py-PDEA$_{30}$–PDMA$_{130}$ system may change the partitioning of nitromethane between the two phases: if the local concentration of Q in proximity to the label is different to that of the nominal bulk concentration added to the solution, then this will influence the resultant k_q as estimated from Eq. (4). Conceivably, the reduction in quenching efficiency observed for the py-PDEA$_{30}$–PDMA$_{130}$/sodium tetraborate solution may not be due to any chain contraction but may merely reflect a change in quencher partitioning between the two phases. In an effort to resolve this issue, the block copolymer dynamics in the presence of buffer were examined *directly* using TRAMS in the next section.

3.2.3. Time-resolved anisotropy measurements

The difference function for py-PDEA$_{30}$–PDMA$_{130}$ when buffered at pH 9 with 0.025 M sodium tetraborate was analysed using impulse reconvolution [46]. Fig. 6b shows $d(t)$ and the associated single exponential fit. The fact that the residuals are randomly distributed around zero and χ^2 is close to unity provide confidence in the quality of the fit. A τ_c of 10.1 ± 1.3 ns results from this analysis. Since a slight increase in τ_c occurs at pH 9 in the presence of buffer when compared to that in the absence of sodium tetraborate (τ_c is *ca*. 1.8 ± 0.2 ns) this implies that the chain ends experience reduced mobility and is consistent with a partial contraction of the chain.

3.3. Monitoring micellization via fluorescence techniques

Since py-PDEA$_{30}$–PDMA$_{130}$ forms stable micelles at pH 9 in the presence of sodium tetraborate buffer, these conditions have been used to study the onset of micellization. In order to achieve this end, the labelled copolymer concentration was kept constant at 0.004 g/l (which is below its CMC, see Fig. 1) and the effect of increasing the concentration of unlabelled Bz-PDEA$_{24}$–PDMA$_{126}$ from below to above the CMC using fluorescence techniques was examined. Under these conditions, intermolecular excimer formation or energy migration between labels is precluded (see Fig. 2), which would otherwise interfere with the anisotropy experiments [44]. We have also monitored the effect of pH on micellar self-assembly. This has been achieved by adding 1.0 g/l of Bz-PDEA$_{24}$–PDMA$_{126}$ to py-PDEA$_{30}$–PDMA$_{130}$ (0.004 g/l) and examining the fluorescence characteristics at various pH values.

3.3.1. Excited state lifetime measurements

Fluorescence decays for py-PDEA$_{30}$–PDMA$_{130}$ (0.004 g/l)/Bz-PDEA$_{24}$–PDMA$_{126}$ (1.0 g/l) were acquired at several pH values. Again, the transient emission was observed to be complex, requiring a minimum of three exponential terms (as in Eq. (2)) for a statistically adequate fit (see Table 1). The average lifetime, calculated *via* Eq. (3) for py-PDEA$_{30}$–PDMA$_{130}$ (0.004 g/l)/Bz-PDEA$_{24}$–PDMA$_{126}$ (1.0 g/l), is also listed for various solution conditions in Table 1. A gradual decrease in $\langle\tau_f\rangle$ occurs as the pH is increased. This is consistent with a decrease in the degree of protonation of the tertiary amines at higher pH. Clearly no micelle formation occurs at pH 1.25: $\langle\tau_f\rangle$ is ~123 ns, which is similar to that observed for pyrene dispersed in water [49]. However, significant interaction occurs at pH 8 ($\langle\tau_f\rangle$ ~48.6 ns): if the $\langle\tau_f\rangle$ observed at pH 8 from py-PDEA$_{30}$–PDMA$_{130}$ (0.004 g/l) is compared with that of py-PDEA$_{30}$–PDMA$_{130}$ (0.004 g/l)/Bz-PDEA$_{24}$–PDMA$_{126}$ (1.0 g/l) at a similar pH (see Table 1), then a decrease is apparent (from *ca*. 97.4 ns to 48.6 ns). This indicates micelle formation, since the local amine concentration has increased through intermolecular interactions between chains, which serve to quench the excited state. Increasing the pH further to pH 9 in the presence of buffer results in a further decrease in $\langle\tau_f\rangle$ to *ca*. 33 ns. One further point is noteworthy from consideration of the data in Table 1: at pH 9.5 the $\langle\tau_f\rangle$ of py-PDEA$_{30}$–PDMA$_{130}$ (0.004 g/l)/Bz-PDEA$_{24}$–PDMA$_{126}$ (1.0 g/l) is *ca*. 27 ns. This can be compared with a $\langle\tau_f\rangle$ of *ca*. 70 ns for py-PDEA$_{30}$–PDMA$_{130}$ (0.004 g/l) under the same pH conditions. In the former case deprotonation is complete and a high local concentration of amines exits through intermolecular interactions in the micelle cores leading to a much shorter lifetime. Clearly, $\langle\tau_f\rangle$ is capable of monitoring the onset of micellization of this diblock copolymer.

3.3.2. Fluorescence quenching

The quenching behaviour of py-PDEA$_{30}$–PDMA$_{130}$ (0.004 g/l) using nitromethane as a quencher was examined in the presence of Bz-PDEA$_{24}$–PDMA$_{126}$ (1.0 g/l) under various solution conditions. The bimolecular quenching data are

listed in Table 2. Inspection of Table 2 reveals that a bimolecular quenching constant of *ca.* 3.51×10^9 mol^{-1} dm^3 s^{-1} was obtained at pH 1.25, which decreased to *ca.* 0.17×10^9 mol^{-1} dm^3 s^{-1} at pH 9 in 0.025 M sodium tetraborate. This latter value can be compared with a bimolecular quenching constant of 0.20×10^9 mol^{-1} dm^3 s^{-1} observed below the CMC at the same pH and buffer concentration. This indicates that it is slightly more difficult for the quencher to access the label once the micelle has formed. Interestingly, when nitromethane was added to py-PDEA$_{30}$–PDMA$_{130}$ (0.004 g/l)/Bz-PDEA$_{24}$–PDMA$_{126}$ (1.0 g/l) at pH 9.5 in the absence of buffer, a k_q value of 1.0×10^9 mol^{-1} dm^3 s^{-1} was obtained (see Table 2). This suggests that the micelles formed under these conditions allow easier access to the core by the quencher. Presumably, this reflects the fact that in the absence of buffer the coronal chains adopt an expanded conformation which, in turn, offers less resistance to a quencher.

3.3.3. Time-resolved anisotropy measurements

When unlabelled Bz-PDEA$_{24}$–PDMA$_{126}$ (1 g/l) was added to py-PDEA$_{30}$–PDMA$_{130}$ (0.004 g/l) at pH 1.25 no significant change in the rate of anisotropy decay was apparent: a τ_c value of 2.7 ± 0.4 ns was derived from impulse reconvolution [46] analyses. This indicates that the mobility of the pyrenyl-labelled block copolymer chain ends is not inhibited under these conditions. This is to be expected, since only highly mobile unimers exist at low pH [38].

In contrast, when unlabelled Bz-PDEA$_{24}$–PDMA$_{126}$ (1.0 g/l) was added to py-PDEA$_{30}$–PDMA$_{130}$ (0.004 g/l) at pH 9 buffered with 0.025 M sodium tetraborate, a marked reduction in the rate of decay of anisotropy was apparent: a τ_c of *ca.* 149 ns (see Table 3) was derived following analysis via a single exponential function of the form of Eq. (5). This can be contrasted with that observed below the CMC from py-PDEA$_{30}$–PDMA$_{130}$ (0.004 g/l) alone in buffer solution: a τ_c of ~21 ns (see Table 3) was derived following modelling with Eq. (5). Anisotropy decays were recorded for py-PDEA$_{30}$–PDMA$_{130}$ (0.004 g/l) as a function of increasing Bz-PDEA$_{24}$–PDMA$_{126}$ concentration. The data resulting from analysis of the single exponential form of Eq. (5) are listed in Table 3. According to Table 3, τ_c increases as the block copolymer concentration increases, reaching a limiting value of *ca.* 200 ns. This indicates that a significant reduction in the mobility of the chain ends occurs during micelle formation. Further examination of Table 3 reveals that no significant change in chain end motion occurs below the CMC (0.007 g/l); a relatively short τ_c (~20 ns) is indicated which is consistent with the formation of unimers under these conditions [38]. This provides evidence that no aggregation of the chains occurs below the CMC. However, at concentrations above the CMC (see Table 3) a dramatic reduction in the mobility of the PDEA-labelled chain ends is apparent (τ_c ~200 ns) as micelle formation occurs. Clearly, TRAMS are capable of monitoring the onset of micellization through the reduction in the mobility of the block copolymer chain ends.

Table 3
Rotational correlation time (τ_c) and corresponding micelle diameter (D) for py-PDEA$_{30}$–PDMA$_{130}$ (0.004 g/l) as a function of Bz-PDEA$_{24}$–PDMA$_{126}$ concentration in 0.025 M sodium tetraborate solution at pH 9 and 20 °C

[Bz-PDEA$_{24}$–PDMA$_{126}$] (g/l)	τ_c (ns)	D (nm)
0	21.4	5.6
0.002	29.4	6.2
0.01	232.2	12.2
0.1	104.1	9.4
1.0	149.5	10.6

For a sphere rotating in a medium of viscosity, η, τ_c is related to its molar volume, V, *via* Eq. (6).

$$\tau_c = \frac{\eta V}{RT} \tag{6}$$

where T is the temperature and R is the gas constant.

If it is assumed that the micelles formed from Bz-PDEA$_{24}$–PDMA$_{126}$ copolymers are hard rotating spheres and that the labelled chain ends are "frozen" within this relatively rigid structure, then motion of the fluorophore should reflect rotation of the micelle itself. The rate of rotation of this sphere will be reflected by τ_c and consequently an estimate of the volume of this rotating entity (and hence its diameter) is possible *via* Eq. (6).

Given a viscosity of 1.002×10^{-3} kg m^{-1} s^{-1} for water at 298 K, the effective particle diameter (D) for each concentration was calculated from the τ_c data listed in Table 3. Interestingly, the particle diameters derived from TRAMS (*ca.* 6 nm, see Table 3) below the CMC are very similar to those as a result of dynamic light scattering and small-angle neutron scattering measurements on PDMA homopolymers [38]. We conclude that, at concentrations less than 0.007 g/l, Bz-PDEA$_{24}$–PDMA$_{126}$ exists as highly mobile unimers. Further examination of the data in Table 3 reveals that the micelle diameter reaches a plateau at *ca.* 12 nm at concentrations above the CMC. This is approximately half that derived for the hydrodynamic diameter from dynamic light scattering measurements on the same sample. There are several possible reasons for the discrepancy between the two techniques.

(i) If the corona is sufficiently fluid/flexible that it does not impart viscous drag on the whole micelle, it could be that the time-resolved anisotropy experiments can only detect rotation of the "hard" micellar core.
(ii) The chain ends are not "frozen" into position when the micelle forms, but a limited degree of mobility occurs due to fluidity within the core itself. A reduced τ_c value would be expected from single exponential analyses of the anisotropy decay under these circumstances. This would thus reduce the mean micelle volume calculated *via* Eq. (6) and the subsequent estimate of the particle diameter.
(iii) The presence of the deprotonated tertiary amines at pH 9 acts as a quencher and reduces both the intensity of fluorescence observed and the duration of the excited state. Indeed, the $\langle \tau_f \rangle$ observed for py-PDEA$_{30}$–PDMA$_{130}$ (0.004 g/l)/Bz-PDEA$_{24}$–PDMA$_{126}$ (1.0 g/l)

when micellization is complete is *ca*. 33 ns. Following 165 ns after excitation ($5 \times \tau_f$) all fluorescence from this sample should have decayed. This places a limit on the timescale that can be accurately followed by TRAMS: the timescale for the chain end mobility within the micelle (*via* τ_c) is close to 200 ns. It is not therefore surprising that the TRAMS estimate of the micelle diameter is subject to a degree of uncertainty (the error is estimated to be ±20%). Within these limitations, a micelle size of 12 nm from TRAMS compared to that of *ca*. 25 nm from dynamic light scattering measurements is perhaps not unreasonable.

Nevertheless TRAMS are capable of detecting the presence of unimers below the CMC and micelle formation at higher block copolymer concentrations. Furthermore, no interactions between labelled py-PDEA$_{30}$–PDMA$_{130}$ chain ends are detected below the CMC, whereas a significant reduction in mobility occurs at higher Bz-PDEA$_{24}$–PDMA$_{126}$ concentrations. In general, the fluorescence data follow the same trend in block copolymer concentration profile as the surface tension measurements.

4. Conclusions

(i) py-PDEA$_{30}$–PDMA$_{130}$ undergoes a conformational change from an expanded chain at pH 1.25 to a partially collapsed state at pH 9 in the presence of 0.025 M sodium tetraborate buffer.

(ii) Protonation of py-PDEA$_{30}$–PDMA$_{130}$ at low pH causes complex quenching behaviour with sodium iodide.

(iii) Deprotonation of this diblock copolymer at high pH results in the formation of tertiary amine groups, which serve as an efficient quencher for the excited state of the label. This provides an additional means by which micellization can be monitored.

(iv) Stern–Volmer experiments suggest that nitromethane quenches the label much less efficiently once the Bz-PDEA$_{24}$–PDMA$_{126}$ micelles have formed.

(v) TRAMS can detect formation of Bz-PDEA$_{24}$–PDMA$_{126}$ micelles since this causes significant reduction in the mobility of the py-PDEA$_{30}$–PDMA$_{130}$ chain ends.

(vi) Time-resolved anisotropy experiments indicate an effective Bz-PDEA$_{24}$–PDMA$_{126}$ micelle diameter of ~12 nm, which is approximately half that obtained from dynamic light scattering measurements. The discrepancy between the two values suggests that the micelle interior is a hard sphere, surrounded by a relatively flexible, fast-moving micelle corona that imparts little viscous drag on the core. However, it is also possible that TRAMS underestimate the micelle size due to the fact that the chain ends are not "frozen"; instead, limited motion occurs due to fluidity within the micelle cores. This is consistent with the low T_g of the PDEA chains [60].

Acknowledgements

The authors gratefully acknowledge support from EPSRC in the form of a post-doctoral fellowship to R.R. Dr. C.D. Vo is also acknowledged for performing the dynamic light scattering measurements.

References

[1] Chu DY, Thomas JK. Macromolecules 1984;17:2142.
[2] Delaire JA, Rodgers MAJ, Webber SE. J Phys Chem 1984;88:6219.
[3] Ghiggino KP, Tan KL. In: Phillips D, editor. Polymer photophysics. London: Chapman and Hall; 1985 [chapter 7].
[4] Chu DY, Thomas JK. J Am Chem Soc 1986;108:6270.
[5] Arora KS, Turro NJ. J Polym Sci Polym Chem Ed 1987;25:259.
[6] Olea AF, Thomas JK. Macromolecules 1989;22:1165.
[7] Winnik FM. Chem Rev 1993;93(2):587.
[8] Soutar I, Swanson L. Macromolecules 1994;27:4303.
[9] Soutar I, Swanson L. ACS Symp Ser 1995;598:388.
[10] Chee CK, Rimmer S, Soutar I, Swanson L. Polymer 2001;42:5079.
[11] Pankasem S, Thomas JK, Snowden MJ, Vincent B. Langmuir 1994;10:3023.
[12] Satguru R, McMahon J, Padget JC, Coogan RG. J Coat Technol 1994;66:47.
[13] Flint NJ, Gardebrecht S, Swanson L. J Fluoresc 1998;8:343.
[14] Soutar I, Swanson L, Annable T, Padget JC, Satgurunathan R. Langmuir 2006;22:5904.
[15] Chee CK, Rimmer S, Soutar I, Swanson L. React Funct Polym 2006;66:1.
[16] Bednar B, Trena J, Svoboda P, Vajda S, Fidler V, Prochazka K. Macromolecules 1991;24:2054.
[17] Binkert T, Oberreich J, Meewes M, Nyffenegger R, Ricka J. Macromolecules 1991;24:5806.
[18] Winnik FM. Polymer 1990;31:2125.
[19] Zhao C-L, Winnik MA, Reiss G, Croucher MD. Langmuir 1990;6:514.
[20] Procházka K, Vajda S, Fidler V, Bednár B, Mukhtar E, Almgren M, et al. J Mol Struct 1990;219:377.
[21] Cao T, Munk P, Ramireddy C, Tuzar Z, Webber SE. Macromolecules 1991;24:6300.
[22] Procházka K, Bednár B, Mukhtar E, Svoboda P, Trená J, Almgren M. J Phys Chem 1991;95:4563.
[23] Rodrigues K, Kausch CM, Kim J, Quirk RP, Mattice WL. Polym Bull 1991;26:695.
[24] Wilhelm M, Zhao C-L, Wang Y, Xu R, Winnik MA, Mura J-L, et al. Macromolecules 1991;24:1033.
[25] Kiserow D, Procházka K, Ramireddy C, Tuzar Z, Munk P, Webber SE. Macromolecules 1992;25:461.
[26] Kiserow D, Chan J, Ramireddy C, Munk P, Webber SE. Macromolecules 1992;25:5338.
[27] Procházka K, Kiserow D, Ramireddy C, Webber SE, Munk P, Tuzar Z. Makromol Chem Macromol Symp 1992;58:201.
[28] Wang Y, Balaji R, Quirk RP, Mattice WL. Polym Bull 1992;28:333.
[29] Frindi M, Michels B, Zana R. J Phys Chem 1992;96:8137.
[30] Chan J, Fox S, Kiserow, Ramireddy C, Munk P, Webber SE. Macromolecules 1993;26:7016.
[31] Duhamel J, Yekta A, Ni S, Khaykin Ya, Winnik MA. Macromolecules 1993;26:6255.
[32] Jada A, Siffert B, Reiss G. Colloids Surf A 1993;75:203.
[33] Wang Y, Kausch CM, Chun M, Quirk RP, Mattice WL. Macromolecules 1995;28:904.
[34] Alexandridis P, Athanassiou V, Hatton TA. Langmuir 1995;11:2442.
[35] Smith CK, Liu G. Macromolecules 1996;29:2060.
[36] Rager T, Meyer WH, Wegner G, Winnik MA. Macromolecules 1997;30:4911.
[37] Creutz S, van Stam J, De Schryver FC, Jerome R. Macromolecules 1998;31:681.

[38] Lee AS, Gast AP, Bütün V, Armes SP. Macromolecules 1999;32:4302.
[39] Gohy JF, Creutz S, Garcia M, Mahltig B, Stamm M, Jerome R. Macromolecules 2000;33:6378.
[40] van Stam J, Creutz S, De Schryver FC, Jerome R. Macromolecules 2000;33:6388.
[41] Matejicek P, Humpolicková J, Procházka K, Tuzar Z, Spirková M, Hof M, et al. J Phys Chem 2003;107:8232.
[42] Bütün V, Billingham NC, Armes SP. Chem Commun 1997:671.
[43] Bütün V, Billingham NC, Armes SP. Polymer 2001;42:5993.
[44] Grazulevicius JV, Soutar I, Swanson L. Macromolecules 1998;31:4820.
[45] Azumi T, McGlyn SP. J Chem Phys 1962;37:2413.
[46] Barkley MD, Kowalczyk AA, Brand L. J Chem Phys 1981;75:3581.
[47] Soutar I, Swanson L, Imhof RE, Rumbles G. Macromolecules 1992;25:4399.
[48] Birks JB. Photophysics of aromatic molecules. London: Wiley-Interscience; 1970.
[49] Ebdon JR, Hunt BJ, Lucas DM, Soutar I, Swanson L, Lane AR. Can J Chem 1995;73:1982.
[50] Chee CK, Rimmer S, Shaw DA, Soutar I, Swanson L. Macromolecules 2001;34:544.
[51] Soutar I, Swanson L. Eur Polym J 1993;29:371.
[52] Winnik MA, Bystryak SM, Liu Z. Macromolecules 1998;31:6855.
[53] Goodpaster JV, McGuffin VL. Anal Chem 2000;72:1072.
[54] Takagishi T, Hosokawa T, Hatanaka Y. J Polym Sci Part A Polym Chem 1989;27:1.
[55] Pradny M, Seveik S. Makromol Chem 1985;186:111.
[56] Kozuka H, Hosokawa T, Takagishi T. J Polym Sci Part A Polym Chem 1989;27:555.
[57] Cao T, Yin W, Armstrong JL, Webber SE. Langmuir 1994;10:1841.
[58] Morrison ME, Dorfman RC, Webber SE. J Phys Chem 1996;100:15187.
[59] Ebdon JR, Lucas DM, Soutar I, Swanson L. Macromol Symp 1994;79:167.
[60] Brandrup J, Immergut EH. Polymer handbook. 3rd ed. New York: Wiley-Interscience; 1989.